International Journal of Thermophysics, Vol. 13, No. 6, 1992

Thermophysical Properties Data on Molten Semiconductors

S. Nakamura[1] **and T. Hibiya**[1]

Received June 2, 1992

Thermophysical properties of molten semiconductors are reviewed. Published data for viscosity, thermal conductivity, surface tension, and other properties are presented. Several measurement methods often used for molten semiconductors are described. Recommended values of thermophysical properties are tabulated for Si, Ge, GaAs, InP, InSb, GaSb, and other compounds. This review shows that further measurements of thermophysical properties of GaAs and InP in the molten state are required. It is also indicated that a very limited amount of data on emissivity is available. Space experiments relating to thermophysical property measurements are described briefly.

KEY WORDS: density; GaAs; GaSb; Ge; high temperature; InP; InSb; molten state; semiconductors; Si; surface tension; thermal conductivity; viscosity.

1. INTRODUCTION

Computer and communication systems play a vital role in the functioning of a modern society. Technologies for these systems have been supported by microelectronics chips, such as ultralarge-scale integrated circuits (ULSI), laser diodes, charge-coupled devices (CCD), etc. These devices are fabricated using high-quality single crystals of silicon, germanium, or compound semiconductors. Most semiconductor single crystals are grown by melt growth methods: Czochralski, floating zone or Bridgman techniques. In these methods, crystal growth is controlled mainly by the heat and mass transfer process at the solid/liquid interface.

Figure 1 shows a cross section of an indium antimonide single crystal grown during Skylab-IV mission [1]. The seed crystal (A) prepared by the

[1] Fundamental Research Laboratories, NEC Corporation, 34 Miyukigaoka, Tsukuba, Ibaraki 305, Japan.

0195-928X/92/1100-1061$06.50/0 © 1992 Plenum Publishing Corporation

Czochralski method on earth shows growth striations, while no striation is observed in the portion (B) grown by the Bridgman method in space. The striation, inhomogeneous impurity distribution, was induced at the solid/liquid interface not only by rotational temperature fluctuation but also by oscillation of the temperature field coupled with time-dependent convection. Figure 1 shows that microgravity in space has a strong effect to suppress convection. Since the rotational temperature distribution is possibly improved, the last unsolved problem is the convection related to

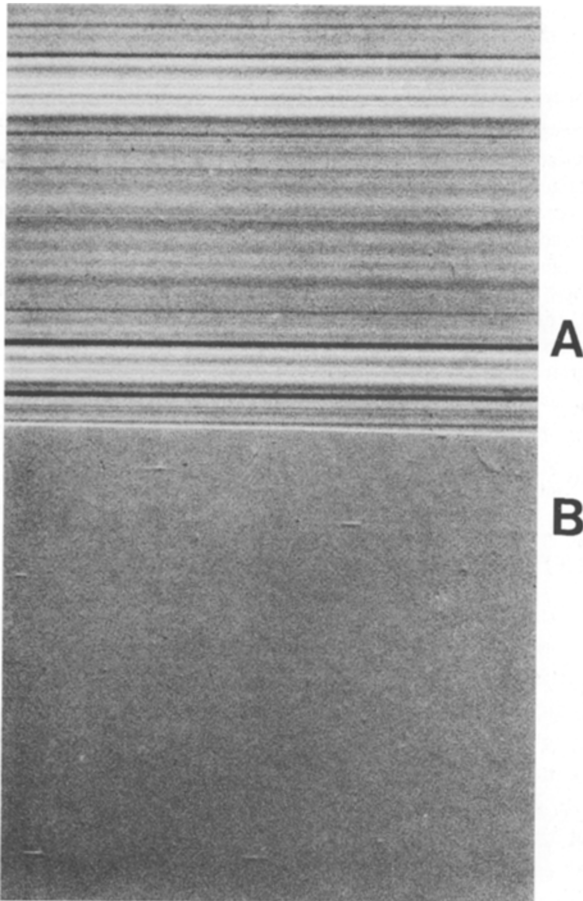

Fig. 1. Cross section of an InSb single crystal grown by the boat technique in a microgravity environment [1]. Portion A was grown on the ground. Portion B was grown suppressing convection under microgravity. (Reprinted by permission from Ref. 1.)

the temperature oscillation. Studying the convection permits us to understand the generation mechanism of the striation and improve the quality of grown crystals.

Convection in a melt is classified into two types: buoyancy and thermocapillary convection. Each type of convection has several modes, such as no flow, stable, oscillatory, and turbulent. Figure 2 shows a map of the buoyancy convection mode, in which the Rayleigh (*Ra*) number is plotted as a function of the Prandtl (*Pr*) number.[2] As shown in Fig. 2, the convection mode for a low Prandtl number liquid is easily converted from no flow to turbulent flow, as proposed by Krishunamurti [2] and Rosenberger and Müller [3]. This suggests that turbulent flow is dominant in a melt during the growth process in most cases. The convection mode was experimentally observed using X-ray radiography by Kakimoto et al. [4]. This work made it possible to compare numerical simulations with experiments. Many simulations of melt convection are considered to be carried out for the comparison. Accurate data on thermophysical properties are required for the simulations.

Computer simulations are effective not only for crystal growth in industries but also for preparation of crystal growth experiments under microgravity, because opportunities for space experiments are very limited

[2] The dimensionless numbers, as well as the notation, are given under Nomenclature.

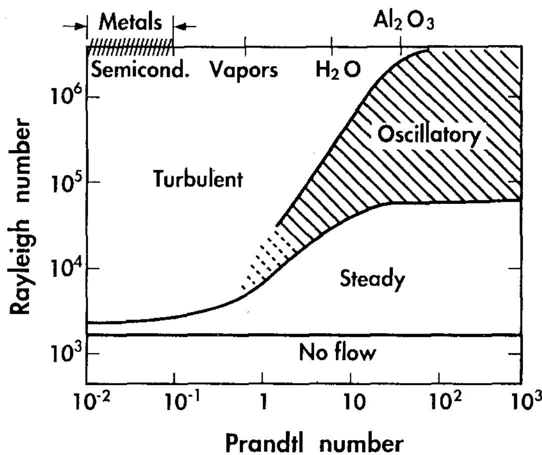

Fig. 2. Regime diagram of convection: For molten semiconductors convection rapidly changes from no flow to turbulent flow [2, 3]. (Reprinted by permission from Ref. 2.)

and space experiments are expensive and time-consuming. In order to perform effective experiments, simulations using accurate thermophysical properties data are definitely necessary.

In addition, the microgravity environment itself is thought to be suitable for measurements of thermophysical properties. Diffusion constants of Sn in molten $Pb_{1-x}Sn_xTe$ [5] and thermal conductivity of molten InSb [6, 7] were measured, since on earth it is usually difficult to measure accurately transport properties of molten semiconductors because of buoyancy convection. In the future, opportunities for experiments in microgravity environment will increase, permitting the development of new experimental techniques for the measurement of thermophysical properties.

The book edited by Glazov et al. [8] was the first monograph on thermophysical properties of molten semiconductors. The density, kinematic viscosity, electrical conductivity, and thermoelectric power were tabulated for elemental semiconductors (Si, Ge), III–V and II–VI compound semiconductors, and others. However, the thermal conductivity and volumetric thermal expansion coefficient were barely mentioned in the monograph. Thermal conductivities of elemental semiconductors and compound semiconductors were reviewed by Regel et al. [9]. Surface tensions of Si and the related compounds were reviewed by Keene [10].

In the present review, we focus on viscosity, thermal conductivity, surface tension, and volumetric thermal expansion coefficient. Emissivity is discussed minimally because of the lack of data. This summary of thermophysical properties including new experimental results should be useful for numerical simulations. These are the main objectives of this review. First, several experimental methods for the measurement of thermophysical properties are considered. Second, thermophysical properties are summarized for silicon and germanium and then for compound semiconductors (III–V, telluride compound semiconductors). Finally, the possibility of space experiments for thermophysical property measurements is reviewed.

2. MEASUREMENT OF THERMOPHYSICAL PROPERTIES OF MOLTEN SEMICONDUCTORS

The high vapor pressure and chemical reactivity of molten semiconductors make it difficult to measure thermophysical properties. A strong affinity to oxygen causes contamination on the surface of molten semiconductors. Since methods of measuring thermophysical properties for molten semiconductors are limited due to the above reasons, there exists

only a limited amount of data on thermophysical properties which have been measured using different experimental methods.

In this section, methods for measuring the thermophysical properties of molten semiconductors are reviewed.

2.1. Viscosity

Although there are several methods for measuring the viscosity of high-temperature melts [11], only the oscillating cup method has often been employed for molten metals [12]. Figure 3 shows a typical apparatus used for the oscillating cup method [13]. A molten sample is contained in a cylindrical crucible which is suspended by a thin elastic wire (molybdenum wire). After torsional oscillation is applied to the crucible, the logarithmic decrement of the oscillation is measured. The decrement is determined by a mirror attached to the wire using a laser beam and two photodiodes. Carbon is often used as crucible material. When this method is applied to molten GaAs, an inner crucible made of pyrolytic boron

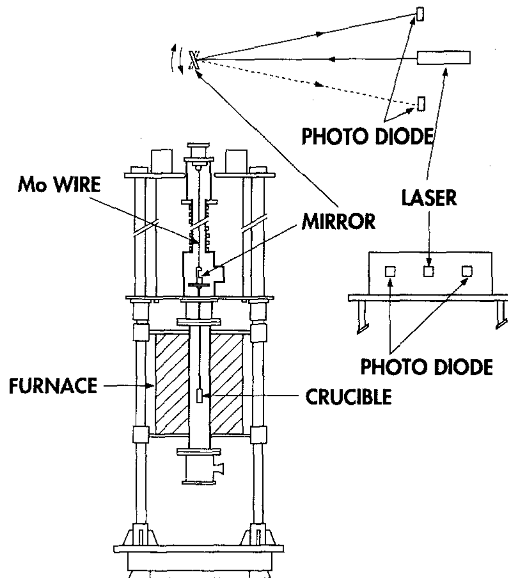

Fig. 3. Oscillating cup method for viscosity measurement [13]. After torsional oscillation is applied to the crucible suspended by an elastic wire, the logarithmic decrement of the oscillation is measured by the reflection of a laser beam using two photo diodes. (Reprinted by permission from Ref. 13.)

nitride (p-BN) with a carbon seal is used to avoid evaporation of As [13–15]. Utilization of such a crucible makes it possible to apply this method to molten semiconductors.

In this method, since a crucible is oscillated, accurate temperature measurement is difficult to achieve by attaching a thermocouple to the crucible. However, viscosity is very sensitive to temperature change near the melting point. It is often seen that viscosity, which is nearly constant at higher temperatures, has a large temperature dependence near the melting point. Measurement by the oscillating cup method is also sensitive to the meniscus shape of a molten sample on the inside wall of the crucible [11]. This depends on the wettability between the sample and the wall.

Figure 4 shows the viscosity of molten semiconductors. There are not many semiconductors whose viscosity has been measured by different researchers [8, 13–20]. For Si and Ge, measured values are in relative agreement with each other. On the other hand, results for compound semiconductors, particularly GaSb, show significant discrepancies. Further measurements on compound semiconductors are needed.

The Andrade formula is often used to relate viscosity with molar volume and atomic weight at a melting point. This formula is an empirical equation which is useful for liquid metals, on the assumption that the characteristic vibration frequency in a liquid and solid state would be the same. Battezzati and Greer [21] determined an Andrade coefficient of 1.88×10^{-7} $(J \cdot K^{-1} \cdot mol^{-1/3})^{1/2}$ for intermetallic compounds. However, except for antimonide compounds, estimated Andrade coefficients for

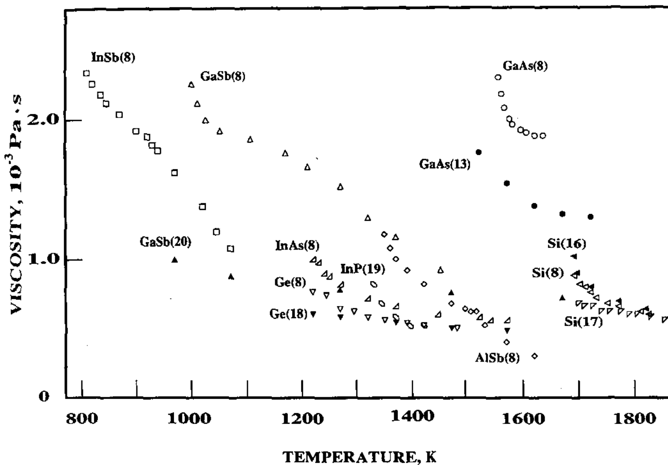

Fig. 4. Dynamic viscosity of molten semiconductors as a function of temperature. Reference numbers are given in parentheses.

molten semiconductors at the melting point seem to be lower values of between 0.4×10^{-7} and 1.0×10^{-7} $(J \cdot K^{-1} \cdot mol^{-1/3})^{1/2}$. These estimated coefficients are similar to the values of silicon and germanium: Si, 0.6×10^{-7} $(J \cdot K^{-1} \cdot mol^{-1/3})^{1/2}$; and Ge, 0.4×10^{-7} $(J \cdot K^{-1} \cdot mol^{-1/3})^{1/2}$ [21]. The lower coefficients for molten semiconductors may be attributed to the assumption that the same vibration frequency for liquid and solid is used to introduce the formula [21].

2.2. Thermal Conductivity

Only a few experimental data exist for thermal conductivity as compared to the other thermophysical properties of molten semiconductors. In addition, there are discrepancies between these data [9]. This is due mainly to the influence of buoyancy convection in molten semiconductors which have a relatively low viscosity. Therefore, the suppression of convection is an important requirement for the measurements of thermal conductivity.

For Si and Ge, thermal conductivities were determined from heat balance at the solid/liquid interface during the Czochralski crystal growth process [22–24]. In this method, the temperature gradient at the interface during the growth process was measured by a thermocouple buried vertically in a grown crystal. Thermal conductivity was determined by solving heat balance equations at the interface [22]. Since the contribution of convection in a melt may not be negligible, values measured with this method seem to be higher than the real values.

Thermal diffusivities of molten Ge, Si, $Pb_xSn_{1-x}Te$, and $Hg_xCd_{1-x}Te$ were determined by the laser flash method [25–29]. In the laser flash method, a short laser pulse strikes the front surface of a thin disk of a molten sample and the rear-face temperature response is recorded by a highly sensitive detecting instrument such as a photopyrometer. Since the temperature response is measured within 1 s, the effect of convection is eliminated. The design of the sample cell is the most crucial problem in the application of this method to molten semiconductors. Figure 5 shows sample cells which have been used for molten $Hg_{1-x}Cd_xTe$ [30]. The disk of a molten sample has a diameter of about 10 mm and a thickness of between 1 and 2 mm in the transparent quartz cell. The details of the procedure for constructing this cell and for synthesizing a molten sample are described in the literature [30]. This kind of measurement cell has enabled application of this method to molten semiconductors.

Measurements of thermal conductivities of molten semiconductors by a transient hot wire method were recently attempted [31, 32]. This technique assures direct measurements but has been conventionally applied to

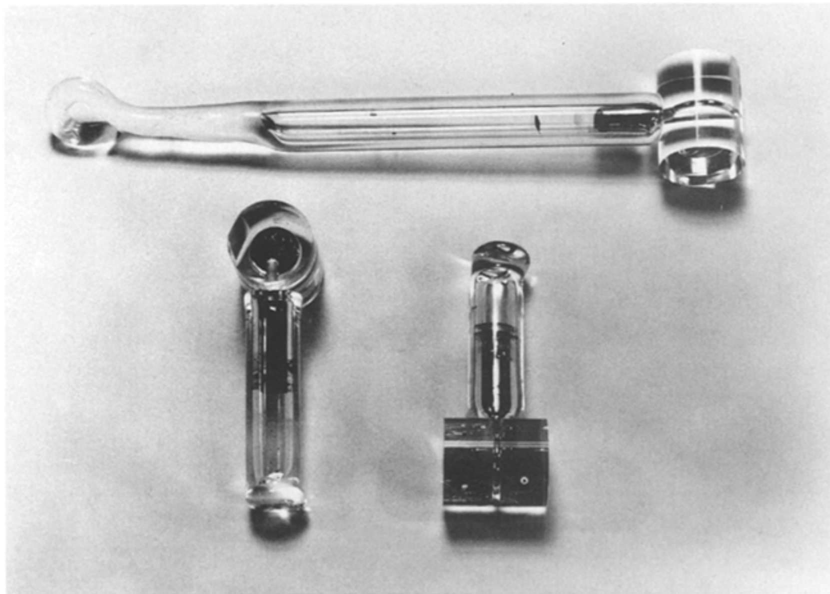

Fig. 5. Sample cell for the laser flash method. Top: The large vapor space in the stem is necessary for loading the sample piece. Bottom: The cells after shortening the stem to reduce vapor volume. The sample disks are shown at the top of the left cell and at the bottom of the right cell [30]. The sample has a 10-mm i.d. (Reprinted by permission from Ref. 30.)

organic materials and gases. As a probe for molten semiconductors, a metallic thin wire was printed on the alumina substrate and insulated with a thin alumina layer. This probe was attached to the molten sample. The temperature increase in the wire was detected when a constant heat input by an electrical current was applied to it. Convection in the molten semiconductors has to be taken into account in this method. This method was successfully applied using an individually developed facility under microgravity on a sounding rocket and in a drop shaft; the thermal conductivity of molten InSb was accurately determined without convection effects [6, 7, 33].

Both the coaxial method and the parallel plates method were used for InSb [34, 35], GaSb [34, 36], and Ge [37, 38i] about 20 years ago. However, recent measurements using these methods have not been found in the literature.

Figure 6 shows the thermal conductivity of molten semiconductors as a function of temperature. Thermal conductivities of Si, Ge, InSb, and GaSb were measured [6, 7, 22–38]. Those of InP and GaAs were estimated [39]. The lack of experimental data is obvious. A molten semiconductor

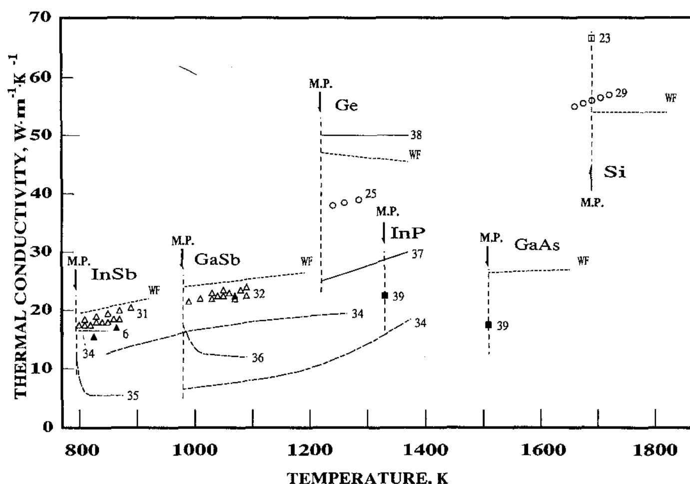

Fig. 6. Thermal conductivity of molten semiconductors. (——) Stationary method; (△) transient hot wire method; (▲) microgravity experiment; (----) coaxial method; (□) heat balance during CZ crystal growth process; (○) laser flash method; (■) estimated value; (----WF) estimated by the Wiedemann–Franz ratio. M.P., melting point. Numbers are reference numbers.

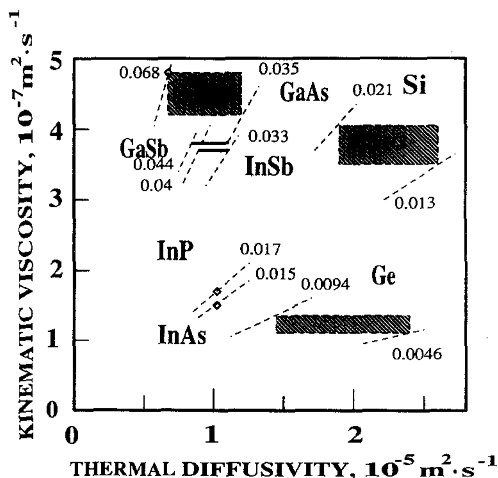

Fig. 7. Kinematic viscosity as a function of thermal diffusivity, Values estimated by Jordan [39] are shown as diamonds. Dashed lines indicate Prandtl numbers. Hatched areas are for silicon, germanium, and gallium arsenide.

has metallic behavior in the molten state. Therefore, the thermal conductivity in the molten state is correlated mostly with the heat conduction due to electrons. Regel et al. [9] showed that the Wiedemann–Franz law is applicable to molten metal and semiconductors. The dashed lines in Fig. 6 were estimated from the Wiedemann–Franz law. Data from recent measurements confirm the estimated values.

Variations of kinematic viscosity as a function of thermal diffusivity as well as Prandtl numbers for several molten semiconductors at the melting point are shown in Fig. 7. Thermal diffusivity is calculated from data on specific heat, density, and thermal conductivity. Kinematic viscosity is also obtained from the experimental results of dynamic viscosity. Since there are several experimental data of thermal diffusivity and kinematic viscosity for Si, Ge, and GaAs, hatched areas in Fig. 7 show possible Prandtl numbers areas for the materials. One-point data were estimated for indium arsenide and indium phosphide [39]. In this figure, slopes indicate Prandtl numbers. The difference of *Pr* would result in variation of flow modes in molten semiconductors.

2.3. Surface Tension

Most measurements of surface tension were performed by the sessile drop method [40, 41], and a few measurements by the drop weight method [42].

For the sessile drop method, surface tension is determined from the shape of the outline of a droplet placed on a horizontal substrate in a furnace. The surface tension is particularly sensitive to oxygen contamination on the melt surface. This was reported for Si by Hardy [43]. In measurements of molten GaAs, surface tension depends on the ambient vapor pressure of As [44]. Therefore, the control of the condition of a molten melt is one of the technically important problems. The value of the surface tension also depends on the substrate material and its surface condition [41].

The drop weight method is much simpler to be carried out than the sessile drop method [42, 45]. A rod of a sample suspended in a vertical furnace is slowly moved into the high-temperature zone. A molten drop is formed at the tip of the rod and the size of the drop is gradually increased. This process is continued until the drop falls off. The surface tension is calculated using the radius of the rod and the weight of the fallen drop. Since the application of this method is limited to the melting temperature of the sample, the temperature coefficient of the surface tension cannot be determined.

Figure 8 shows the surface tension of silicon, germanium, and gallium

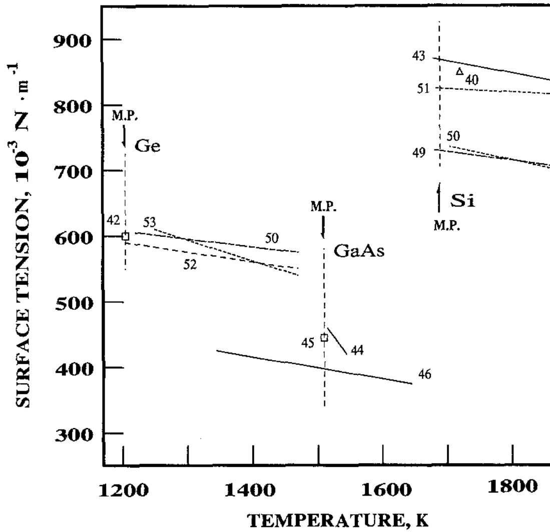

Fig. 8. Surface tension of silicon, germanium, gallium arsenide, and indium arsenide. Measurements were performed by the sessile drop method or drop weight method. Dashed vertical lines indicate melting points. Numbers indicate references.

arsenide in the molten state [11, 40–53]. Various data on germanium are in agreement with each other. Data on silicon depend on the atmosphere; higher values were obtained in an atmosphere with a lower oxygen concentration. Temperature coefficients for Si and Ge may be determined experimentally. On the other hand, even absolute values for GaAs are not yet certain.

2.4. Density and Volumetric Thermal Expansion Coefficient

For the measurement of density, a hydrostatic weight method and a maximum-bubble pressure method have been used. These methods are described in detail in the literatures [8, 54].

The volumetric thermal expansion coefficient, β, is obtained from the temperature coefficient of density ρ, as follows [54, 55]:

$$\beta = -\frac{1}{\rho}\frac{d\rho}{dT} \tag{1}$$

Existing data on several compound semiconductors may not be sufficient to determine density reliably. For example, the value for gallium arsenide is determined from only two data points of density. On the other

hand, the coefficients for silicon and germanium are considered to be more reliable than those for compound semiconductors, because there are several data on density for Si and Ge [54].

2.5. Other Properties

Measurements of the Hall coefficient and carrier concentration in molten III–V compounds were performed by Glazov et al. [56, 57]. Carrier concentrations were about 10^{22} to $10^{23}\ cm^{-3}$. In general, III–V compounds show metallic behavior in the molten state. Free electron approximation is a reasonably good scheme to understand the nature of the molten state.

Compressibilities were determined from absorption of sound in molten semiconductors [58–60]. The specific heats of some molten semiconductors were determined from thermal measurements [61–63].

Emissivity (hemispheric total) may be one of the important thermophysical properties controlling heat transfer in the crystal growth process, as long as radiation heat transfer is concerned. However, there are no data for compound semiconductors. An emissivity of 0.27 is used for silicon [64].

3. THERMOPHYSICAL DATA FOR SILICON AND GERMANIUM

3.1. Silicon

Thermophysical properties of molten silicon are the most widely investigated. Nevertheless, all the properties are not accurately known. Table I shows thermophysical properties of molten silicon. Data on viscosity [16], surface tension [43], thermal conductivity [29], and Hall coefficient [57] represent recent measurements.

Density was measured with various methods and the data are in a reasonable agreement [8, 54]. The volumetric thermal expansion coefficient was determined using Eq. (1) by incorporating the density data. For volumetric expansion coefficient, two different values had been reported, $1.43 \times 10^{-4}\ K^{-1}$ [8, 54] and $1.43 \times 10^{-5}\ K^{-1}$ [65]. Recently Kakimoto et al. [66] performed checks on the validity of the two numbers. Calculated velocity and flow pattern were identical to those experimentally observed by an X-ray radiography technique [4], when $\beta = 1.43 \times 10^{-4}$ was used. Therefore, a volume expansion coefficient of the order of 10^{-4} is recommended.

Viscosioty was tabulated by Glazov et al. [8] and also measured by Turovsky and Lyubimov [17] and Kakimoto et al. [16], as shown in

Table I. Thermophysical Properties of Silicon and Germanium

Property	Unit	Silicon	Ref. No.	Germanium	Ref. No.
Density (ρ)	$kg \cdot m^{-3}$	2.52×10^3	8, 54	5.49×10^3 [a]	8
				5.51×10^3	54
Specific heat (C_p)	$J \cdot g^{-1} \cdot K^{-1}$	1.037	64	0.379	61
Dynamic viscosity (μ)	$Pa \cdot s$	0.88×10^{-3}	8	0.74×10^{-3}	8
		0.63×10^{-3}	17	0.61×10^{-3}	18
		1.02×10^{-3}	16		
Thermal conductivity (λ)	$W \cdot m^{-1} \cdot K^{-1}$	56 [a]	29	38.7 [a]	25
		66.9	24	25	37
				50	38
				71.1	22
Surface tension (γ)	$N \cdot m^{-1}$	874×10^{-3} [a]	43	600×10^{-3}	42
		860×10^{-3}	40		
		720×10^{-3}	42		
Volumetric thermal expansion coefficient (β) [b]	K^{-1}	1.43×10^{-4}		0.94×10^{-4} [a]	
				1.18×10^{-4}	
Compressibility	$m^2 \cdot N^{-1}$	2.6×10^{-11}	58	2.5×10^{-11}	59

[a] Recommended value.
[b] Calculated by author.

Fig. 4. All these measurements were performed by the oscillating cup method. The dynamic viscosity has similar values above 1780 K. However, data of Turovsky and Lyubimov were lower than the others near the melting point. This may be due to the purity difference of molten silicon as explained by Glazov et al. [8] or due to a surface "film" as explained by Turovsky and Ivanova [18] for measurements on germanium.

The data obtained by Glazov et al. [8] showed that the logarithm of kinematic viscosity as a function of inverse temperature had a linear relationship at high temperatures. The tangent to the function is the activation energy of viscous flow. With decreasing temperature toward the melting point, the logarithm of kinematic viscosity deviates from the linear relationship. This means that the activation energy at high temperatures was almost constant, but it increased with decreasing temperature to the melting point. This may suggest a structural change in molten silicon near the melting point [8].

Among the thermophysical properties of molten silicon, surface tension is measured most. However, most measurements were carried out

by the sessile drop method. The surface tension at 1723 K obtained by Hardy [43] in an atmosphere of Ar was 874×10^{-3} $N \cdot m^{-1}$, which was higher than previous data (700×10^{-3} to 750×10^{-3} $N \cdot m^{-1}$) [49–51]. Hardy [43] showed that the surface tension progressively decreased with increasing oxygen leakage into the measurement system. This suggested that the previous data may be influenced by oxygen contamination on the surface of molten silicon.

The temperature coefficient of surface tension is required to simulate the Marangoni convection, which is a melt surface flow due to surface tension gradient. The value -0.28×10^{-3} $N \cdot m^{-1} K^{-1}$ reported by Hardy [43] may be recommended. The temperature coefficient apparently increases as the measured surface tension increases, suggesting that the coefficient decreases with increasing oxygen concentration. Therefore, it is necessary to measure surface tension as a function of oxygen partial pressure [10].

The widely accepted thermal conductivity 66.9 $W \cdot m^{-1} \cdot K^{-1}$ was measured by a heat balance method during a CZ crystal growth process [23, 24], as described in Section 2.2. Yamamoto et al. [29] recently measured the thermal conductivity using a laser flash method. The value of thermal conductivity was 56 $W \cdot m^{-1} \cdot K^{-1}$ at the melting point in the liquid state. The result of the Hall coefficient measurement indicated that molten silicon is metallic. On the assumption of a free electron model, the calculated carrier density was 2.3×10^{22} cm^{-3}, which was similar to that of a typical liquid metal [58]. The thermal conductivity estimated by the Wiedemann–Franz law was 49.6 $W \cdot m^{-1} \cdot K^{-1}$ using the data of electrical conductivity [8]. This estimated value is in reasonable agreement with the recent value measured by the laser flash method [29].

3.2. Germanium

Since the melting point of germanium is lower than that of silicon, thermophysical properties of molten germanium have been investigated in more detail. The recommended thermophysical properties of molten Ge at the melting point are shown in Table I.

Density measurements were reviewed by Lucas [54]. The data were in agreement with those of Glazov [8]; volume expansion coefficients were 0.94×10^{-4} K^{-1} [54] and 1.18×10^{-4} K^{-1} [8].

Viscosity was measured by Glazov et al. [8] and by Turovsky and Ivanova [18]. The temperature dependencies of their results are very similar to that of silicon. The viscosities were in reasonable agreement with each other at higher temperatures. However, near the melting point, the

viscosity measured by Turovsky and Ivanova was lower than that of Glazov et al.

Several results of the thermal conductivity disagree. Thermal conductivity measured from heat balance in CZ crystal growth was $71.1\ \mathrm{W \cdot m^{-1} \cdot K^{-1}}$ [22]. Thermal conductivities measured by Glazov et al. [37] and Filippov et al. [38] using steady-state methods were 25 and $50\ \mathrm{W \cdot m^{-1} \cdot K^{-1}}$, respectively. The thermal diffusivity of germanium was recently measured with a laser flash method by Crouch et al. [25]; thermal conductivity calculated from the thermal diffusivity was $38.7\ \mathrm{W \cdot m^{-1} \cdot K^{-1}}$ at the melting point. Thermal conductivity estimated by the Wiedemann–Franz law was $48.4\ \mathrm{W \cdot m^{-1} \cdot K^{-1}}$ [67]. We believe that the value of $71.1\ \mathrm{W \cdot m^{-1} \cdot K^{-1}}$ for thermal conductivity, which has been often used, may be higher than the true value. A value of $38.7\ \mathrm{W \cdot m^{-1} \cdot K^{-1}}$ is recommended for the thermal conductivity of germanium until further data become available.

Although new measurements of the surface tension could not be found, the previous data were in good agreement with each other. The surface tension at the melting point is $600 \times 10^{-3}\ \mathrm{N \cdot m^{-1}}$ [42]. The data of surface tension are in much better agreement compared to those of molten silicon. The reason for this may be due to the smaller effect of oxygen contamination on molten germanium [11].

4. THERMOPHYSICAL PROPERTIES DATA ON COMPOUND SEMICONDUCTORS

4.1. Gallium Arsenide

Fewer measurements of thermophysical properties exist for molten GaAs compared to those for silicon or germanium. This is apparently due to the chemical reactivity in the molten state and the high vapor pressure of arsenic. The thermophysical properties of molten GaAs are shown in Table II. Measurements of density [8], viscosity [8, 13–15], and surface tension [44–47] were performed. The specific heat [63, 39] and thermal conductivity [39] were estimated. The volume expansion coefficient was calculated using Eq. (1) with only two data points of density.

Viscosity was measured by Glazov et al. [8] and by Kakimoto and Hibiya [13] using the oscillating cup method. As shown in Fig. 4, the viscosity given by Kakimoto and Hibiya increases rapidly with decreasing temperature near the melting point. Figure 9 shows the composition dependence of viscosity for molten $Ga_{1-x}As_x$ ($0.0 < x < 0.53$), which shows a peak at stoiciometric composition just above the melting point [13]. This peak decreases with increasing temperature. These data seem to

Table II. Thermophysical Properties of Gallium Arsenide and Indium Phosphide

Property	Unit	GaAs	Ref. No.	InP	Ref. No.
Density (ρ)	$kg \cdot m^{-3}$	$5.71 \times 10^{3\,a}$ 5.99×10^3	8 45	6.03×10^3	19
Specific heat (C_p)	$J \cdot g^{-1} \cdot K^{-1}$	0.434^b	39	0.424^b	39
Dynamic viscosity (μ)	$Pa \cdot s$	1.81×10^{-3} 4×10^{-3}	8 13	0.801×10^{-3}	19
Thermal conductivity (λ)	$W \cdot m^{-1} \cdot K^{-1}$	17.8^b	55	22.8^b	39
Surface tension (γ)	$N \cdot m^{-1}$	$470 \times 10^{-3\,a}$ 442×10^{-3} 401×10^{-3}	44 45 46	385×10^{-3}	48
Volumetric thermal expansion coefficient (β)[c]	K^{-1}	1.84×10^{-4}		4.44×10^{-4}	

[a] Recommended value.
[b] Estimated value.
[c] Calculated by author.

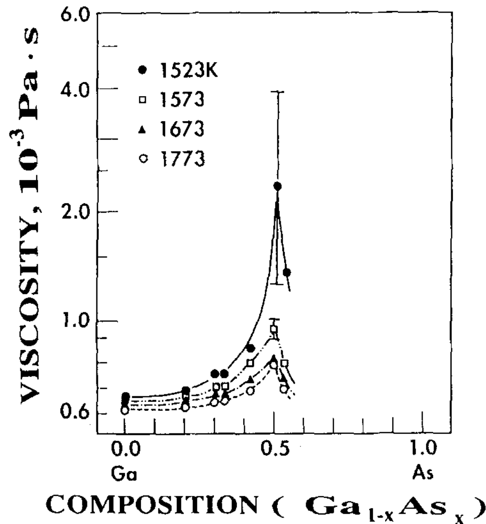

Fig. 9. Composition dependence of the viscosity of molten $Ga_{1-x}As_x$ ($0 < x < 0.53$) in the temperature range from 1250 and 1500°C. The steep increase in viscosity at the stoichiometric composition may be related to the existence of chemical bonding and short-range ordering in a molten state [14]. (Reprinted by permission from Ref. 14.)

indicate the existence of some structure in molten GaAs near the melting point.

The measurements of the surface tension were performed by the sessile drop method [44] and the drop weight method [45]. The surface tension measured by the drop weight method was $442 \times 10^{-3}\ N \cdot m^{-1}$ at the melting point [45]. This surface tension was obtained using a density of $5.99 \times 10^3\ kg \cdot m^{-3}$. Other values of surface tensions were correlated to a density of $5.71 \times 10^3\ kg \cdot m^{-3}$. The surface tension by the sessile drop method was $470 \times 10^{-3}\ N \cdot m^{-1}$ at the melting point and decreased with increasing temperature [44]. However, their value of the temperature coefficient for the surface tension seems to be rather large. Rupp and Müller [46] also measured the surface tension, improving the arsenic vapor pressure condition in the measurement cell. They determined the surface tension to be $401 \times 10^{-3}\ N \cdot m^{-1}$ and its temperature coefficient $-0.18 \times 10^{-3}\ N \cdot m^{-1}\ K^{-1}$. The temperature coefficient of $-0.24 \times 10^{-3}\ N \cdot m^{-1} \cdot K^{-1}$ was calculated recently by Monte Carlo simulations [68]. It was experimentally found that the value of the surface tension depends on the substrate material and surface condition and on the amount of excess As [44].

Amashukeli [47] measured the interfacial tension of a molten GaAs drop on a substrate immersed in molten boric oxide. The interfacial condition of this experiment was similar to that of an actual liquid-encapsulated Czochralski process. The value of the interfacial tension was $500 \times 10^{-3}\ N \cdot m^{-1}$.

The thermal conductivity of molten GaAs has not been experimentally determined. Jordan [39] estimated the thermal conductivity on the assumption that the raio of thermal conductivity of the liquid state to that of the solid state at the melting point is 2.5; this assumption was derived from the experimental results for Si, Ge, InSb, and GaSb. This estimated thermal conductivity of molten GaAs is $17.8\ W \cdot m^{-1} \cdot K^{-1}$. Although it is not clear whether the Wiedemann–Franz law is applicable to molten GaAs, thermal conductivity estimated by this law is $29.2\ W \cdot m^{-1} \cdot K^{-1}$. The specific heat was estimated to be $0.434\ J \cdot g^{-1} \cdot K^{-1}$ by Jordan [39].

4.2. Indium Phosphide

The thermophysical properties of indium phosphide are shown in Table II. The properties are scarce due to the high vapor pressure of phosphorus. Only density, viscosity, and surface tension were experimentally determined [19, 48].

The density results of Glazov et al. [19] suggested that thermal

dissociation has a minor influence on the short-range order structure close to the melting point.

The volume expansion coefficient calculated by the authors using Eq. (1) is $4.44 \times 10^{-4}\ K^{-1}$. The specific heat and thermal conductivity were estimated to be $0.424\ J \cdot g^{-1} \cdot K^{-1}$ and $22.8\ W \cdot m^{-1} \cdot K^{-1}$, respectively, by the same approximation as used for molten gallium arsenide [39]. Since no electrical conductivity and Hall coefficient measurements are reported, thermal conductivity could not be estimated by the Wiedemann–Franz law. A value of $385 \times 10^{-3}\ N \cdot m^{-1}$ for the surface tension in an atmosphere of 27.5 atm phosphorus pressure was determined by Popov and Demberel [48] by the drop weight method.

4.3. Indium Antimonide and Gallium Antimonide

Table III summarizes the thermophysical properties of indium and gallium antimonides. The temperature dependencies of the viscosity of antimonide compounds measured by Glazov et al. [8] were different from those of other molten semiconductors, as shown in Fig. 4. The viscosity displays different temperature dependencies in adjacent temperature regions. However, recent data of Kakimoto and Hibiya [20] were much lower and its temperature dependence was quite simple. Viscosity should be measured again to overcome these discrepancies.

Presently, viscosities of Ga, Sb, and GaSb were measured by Kakimoto and Hibiya [20]. The viscosity for molten GaSb was higher

Table III. Thermophysical Properties of Gallium Antimonide and Indium Antimonide

Property	Unit	InSb	Ref. No.	GaSb	Ref. No.
Density (ρ)	$kg \cdot m^{-3}$	6.48×10^3	8	6.03×10^3	8
Specific heat (C_p)	$J \cdot g^{-1} \cdot K^{-1}$	0.283	62	0.328	62
Dynamic viscosity (μ)	$Pa \cdot s$	2.34×10^{-3}	8	2.26×10^{-3}	8
				1.00×10^{-3}	20
Thermal conductivity (λ)	$W \cdot m^{-1} \cdot K^{-1}$	17.7[a]	32	21.7	32
		12.3	35	17.8	36
		17.1	34		
Surface tension (γ)	$N \cdot m^{-1}$	290×10^{-3}	69	440×10^{-3}	46
Volumetric thermal expansion coefficient (β)[b]	K^{-1}	9.81×10^{-5}		9.58×10^{-5}	

[a] Recommended value.
[b] Calculated by author.

than the average value of molten Ga and Sb near the melting point [20]. However, at a higher temperature, the viscosity was the same as the averaged value. This suggests that near the melting point, some structure can exist in the molten state. However, at high temperatures the structure may disappear and become similar to metallic structure. A kinetic study was also carried out by measuring the viscosity change during a direct synthesis of GaSb; Before the measurement, solid gallium (melting point $T_m = 300$ K) and antimony ($T_m = 700$ K) were separated with thin GaSb disks ($T_m = 985$ K) in a measurement cell. The temperature was elevated up to the melting point of the solid GaSb disk, which prevented mixing of the Ga and Sb melts. When GaSb began to melt, measurements of viscosity were started. By observing the viscosity change with elapsed time, the reaction process of the metal elements was observed. The activation energy of this reaction was determined to be 64.8×10^3 J $\cdot$ mol^{-1}.

The thermal conductivity of InSb [35] and GaSb [36] measured by a stationary method showed an abrupt decrease just above the melting temperature. However, no such sharp decrease was observed in the measurements by Nakamura et al. [6, 7] and Fedorov and Machuev [34]. In measurements with the transient hot wire method, the thermal conductivity of InSb and GaSb increased slightly with increasing temperature. These results showed that the Lorenz number determined by the Wiedemann–Franz law was near the Sommerfeld number, suggesting that molten InSb is metallic near the melting point [32].

A value of 290×10^{-3} N $\cdot$ m^{-1} for the surface tension of indium antimonide was determined from the equilibrium shape of molten zones in the floating zone method [69].

4.4. Telluride Compounds

The thermophysical properties of $Hg_{1-x}Cd_xTe$ and $Pb_{1-x}Sn_xTe$ are investigated mainly for the purpose of space experiments. It was found that the thermal diffusivities of $Hg_{1-x}Cd_xTe (0 < x < 0.3)$, $Cd_{0.96}Zn_{0.04}Te$, PbTe, and PbSnTe were measured by a laser flash method. The thermal diffusivity of $Hg_{1-x}Cd_xTe$ increases with increasing temperature and decreasing x composition.

Density and viscosity of telluride compounds are summarized by Glazov et al. [8]. The surface tension of CdTe and $Pb_{0.8}Sb_{0.2}Te$ was measured by the sessile drop method [41, 70]. Other thermophysical properties for $Pb_{0.8}Sb_{0.2}Te$ are summarized in the literature [70].

5. THERMOPHYSICAL DATA AND MICROGRAVITY

A microgravity environment, where gravity is reduced to 10^{-4}–10^{-6} g compared with that on the earth, is a new frontier of thermophysical property measurements. In a microgravity environment, buoyancy convection is expected to be suppressed to a great extent. This effect of convection suppression is very significant for measurements of several thermophysical properties, particularly for liquids with low Prandtl numbers, such as molten semiconductors and metals.

The diffusion constant measurement of molten Sn was first achieved in a microgravity environment [71]. The measurements on board the space shuttle SL-1 and D-1 flights showed that the Ahrenius equation cannot be applied to the diffusion constant of molten Sn, but the diffusion constant is proportional to the square of the absolute temperature. Diffusion constant measurement of Sn in molten $Pb_{1-x}Sn_xTe$ was carried out on board the TEXUS sounding rocket [5]. As mentioned in Section 4.3, thermal conductivity is strongly influenced by buoyancy convection. The thermal conductivity of molten InSb was measured under microgravity conditions [6, 7], which clearly indicated the suppression of buoyancy convection.

A new measurement facility for thermophysical properties is being planned (TEMPUS: German space experiment facility for containerless processing using electromagnetic positioning and inductive heating under an ultrahigh vacuum) [72]. This will offer opportunities to measure several thermophysical properties of molten materials under microgravity. Surface tension will be obtained by analyzing the shape oscillation of a levitated molten sample when the sample is deformed by electromagnetic forces. Viscosity will also be determined by measuring the damping rate of the oscillation. Measurement of specific heat can be also performed. It is noteworthy that thermophysical properties of an undercooled melt can be evaluated using this technique, since this technique needs no crucible whose wall causes nucleation and contamination.

Even under a microgravity environment, thermocapillary convection (Marangoni convection) occurs due to the surface tension gradient of a molten sample. Therefore, recent measurements of the surface tension were motivated for the purpose of estimating Marangoni convection in space experiments [43–46]. On the other hand, critical Marangoni numbers were experimentally determined from crystal growth experiments; the critical Marangoni number is defined as a number above which Marangoni convection becomes oscillatory. The critical Marangoni numbers for molten Si and GaAs are 200 [73] and 600 [46], respectively.

6. CONCLUDING REMARKS

The knowledge of thermophysical data of molten semiconductors is quite limited, as indicated in this review. Among the thermophysical properties, emissivity is believed to be one of the most indispensable, because radiation heat transfer in the crystal growth process can be described by emissivity. However, the data are apparently lacking, while a levitation technique has been applied to the measurement for molten metals [74]. Further measurements are necessary for emissivity as well as for other properties.

We emphasize in this review that the properties should be used by taking into account the reliability of these data. Attention should be also paid to the measurement principles, working equations, measurement conditions, and physical meaning of measured values. In this review, we have described that the thermophysical properties are parameters to be used for numerical simulations. However, by numerical simulations, the data of thermophysical properties themselves could be evaluated or the reliability of the property could be checked. A numerical simulation with several varying thermophysical properties was performed [65, 75].

Monte Carlo simulations may predict thermophysical properties [68, 76, 77]. The calculated surface tension of GaAs was in reasonable agreement with the experimental results [68].

In the future, the study of thermophysical properties may first focus on the structural change in a melt, as indicated by viscosity and other properties' measurements. The melt structure seems to be related to thermophysical properties.

NOMENCLATURE

ρ	Density
C_p	Specific heat
ν	Kinematic viscosity
μ	Dynamic viscosity $\mu = \nu\rho$
κ	Thermal diffusivity
λ	Thermal conductivity $\lambda = \kappa C_p \rho$
β	Volumetric thermal expansion coefficient
γ	Surface tension
$d\gamma/dT$	Temperature coefficient of surface tension
g	Gravitational acceleration
T	Temperature
ΔT	Temperature difference
L	Characteristic dimension

$$\text{Prandtl number, } Pr = \frac{\nu}{\kappa}$$

$$\text{Rayleigh number, } Ra = \frac{gT\beta L^3}{\nu\kappa}$$

$$\text{Marangoni number, } Ma = \frac{(d\gamma/dT)\,\Delta TL}{\kappa\mu}$$

REFERENCES

1. A. F. Witt, H. C. Gatos, M. Lichtensteiger, M. C. Lavine, and C. J. Herman, *J. Electrochem. Soc.* **122**:276 (1975).
2. R. Krishunamurti, *J. Fluid Mech.* **60**:285 (1973).
3. F. Rosenberger and G. Müller, *J. Crystal Growth* **65**:91 (1983).
4. K. Kakimoto, M. Eguchi, H. Watanabe, and T. Hibiya, *J. Crystal Growth* **88**:365 (1988).
5. M. Katayama, M. Kaneko, T. Horitomi, Y. Nakagawa, and L. Auguste, *Proc. XI Jpn. Symp. Thermophys. Prop.* (1990), p. 219.
6. S. Nakamura, T. Hibiya, F. Yamamoto, and T. Yokota, *Int. J. Thermophys.* **12**:783 (1991).
7. S. Nakamura and T. Hibiya, *Proc. 8th Eur. Symp. Mater. Fluid Sci. Micrograv.* (1992) (in press).
8. V. M. Glazov, S. N. Chizhevskaya, and N. N. Glagoleva, *Liquid Semiconductors* (Plenum Press, New York, 1969).
9. A. R. Regel, I. A. Smirnov, and E. V. Shadrichev, *Phys. Stat. Sol.* **5**:13 (1971).
10. B. J. Keene, *Surface Interface Anal.* **10**:367 (1987).
11. A. Nagashima, *Int. J. Thermophys.* **11**:417 (1990).
12. J. M. Grouvel and J. Kestin, *Appl. Sci. Res.* **34**:427 (1987).
13. K. Kakimoto and T. Hibiya, *Appl. Phys. Lett.* **50**:1249 (1987).
14. K. Kakimoto and T. Hibiya, *Appl. Phys. Lett.* **52**:1576 (1988).
15. S. Ozawa, M. Eguchi, T. Fujii, and T. Fukuda, *Appl. Phys. Lett.* **51**:197 (1987).
16. K. Kakimoto, M. Eguchi, H. Watanabe, and T. Hibiya, *J. Crystal Growth* **94**:412 (1989).
17. B. M. Turovsky and A. P. Lyubimov, *Izv. VUZov, Chern. Metallurg.* **1**:24 (1960).
18. B. M. Turovsky and I. I. Ivanova, *Zhur. Ziz. Khim.* **45**:176 (1971).
19. V. M. Glazov, K. Dovletov, A. Ya. Nashelškii, and M. M. Mamedov, *Neorg. Mater.* **13**:34 (1977).
20. K. Kakimoto and T. Hibiya, *J. Appl. Phys.* **66**:4181 (1988).
21. L. Battezzati and A. L. Greer, *Acta Metall.* **37**:1791 (1989).
22. J. C. Brice and P. A. C. Whiffin, *Solid-State Electron.* **7**:183 (1964).
23. M. G. Milvidskii and V. V. Eremeev, *Sov. Phys. Solid State* **6**:1549 (1965).
24. Yu. M. Shashkov and V. P. Grishin, *Sov. Phys. Solid State* **8**:447 (1966).
25. R. K. Crouch, A. L. Fripp, W. J. Debnam, R. E. Taylor, and H. Groot, in *Materials Processing in the Reduced Gravity Environment of Space*, G E. Rindone, Ed. (North-Holland, Amsterdam, 1983), p. 657.
26. R. E. Taylor, L. R. Holland, and R. K. Crouch, *High Temp.-High Pres..* **17**:47 (1985).
27. L. R. Holland and R. E. Taylor, *J. Vac. Sci. Technol.* **A1**:1615 (1983).
28. S. Sen, W. H. Konkel, S. J. Tighe, L. G. Bland, S. R. Sharma, and R. E. Taylor, *J. Cryst. Growth* **86**:111 (1988).
29. K. Yamamoto, T. Abe, and S. Takasu, *Jpn J. Appl. Phys.* **30**:2423 (1991).
30. L. R. Holland, R. P. Harris, and R. Smith, *Rev. Sci. Instrum.* **54**:993 (1983).
31. S. Nakamura, T. Hibiya, and F. Yamamoto, *Int. J. Thermophys.* **9**:933 (1988).

32. S. Nakamura, T. Hibiya, and F. Yamamoto, *J. Appl. Phys.* **68**:5125 (1990).
33. F. Yamamoto, S. Nakamura, T. Hibiya, T. Yokota, D. Grothe, H. Harms, and P. Kyr, *Proc. CSME Mech. Eng. Forum* (1990), p. 1.
34. V. I. Fedorov and V. I. Machuev, *Teplofiz. Vysokikh Temp.* **8**:447 (1970).
35. Kh. I. Amirkhanov and Ya. B. Magomedov, *Sov. Phys. Solid State* **7**:506 (1965).
36. Kh. I. Amirkhanov and Ya. B. Magomedov, *Sov. Phys. Solid State* **8**:241 (1966).
37. V. M. Glazov, A. A. Aaivazov, and V. G. Pavlov, *Sov. Phys. Semicond.* **5**:182 (1971).
38. L. P. Filippov, A. V. Arutyunov, I. N. Makarenko, I. P. Mardyking, L. I. Trukhanova, B. I. Khusainova, and R. P. Yurchak, *Heat and Mass Transport* (Nauki i Teknika, Minsk (1968), p. 7.
39. A. S. Jordan, *J. Cryst. Growth* **71**:551 (1985).
40. W. D. Kingery and M. Humenik Jr., *J. Phys. Chem.* **57**:359 (1953).
41. R. Shetty, R. Balasubramanian, and W. R. Wilcox, *J. Cryst. Growth* **100**:51 (1990).
42. P. H. Keck and W. V. Horn, *Phys. Rev.* **91**:512 (1953).
43. S. C. Hardy, *J. Cryst. Growth* **69**:456 (1984).
44. R. Shetty, R. Balasubramanian, and W. R. Wilcox, *J. Cryst. Growth* **100**:58 (1990).
45. V. V. Karatev, M. G. Milv̆idskii, and N. Ya. Zakharova, *Iz. Akad. Nauk SSSR Neorgan. Mater.* **2**:833 (1966).
46. R. Rupp and G. Müller, *J. Cryst. Growth* **113**:131 (1991).
47. M. D. Amashukeli, V. V. Karataev, M. G. Kekua, M. G. Milv̆idskii, and D. V. Khantadze, *Neorgan. Mater.* **17**:2126 (1981).
48. A. S. Popov and L. Demberel, *Krist. Tech.* **12**:1167 (1977).
49. S. V. Lukin, V. I. Zhuchkov, N. A. Vatolin, and Y. S. Kozlov, *J. Less Common Metals* **67**:407 (1979).
50. F. N. Tav̆adze, M. G. Kekua, D. V. Khantadze, T. G. Tsertsvade, in *Poverkh. Yavleniya Rasplavakh* N. N. Eremenko, (ed.) (Naukova Dumka, Kíev, 1968), p. 159.
51. V. N. Bobkovski, V. I. Kostikov, V. Y. Levin, and A. S. Tarabanov, *Konstr. Mater. Osn. Grafita* **5**:138 (1970).
52. M. Brunet, J. C. Joud, N. Eustathopoulos, and P. Desre, *J. Less Common Metals* **51**:69 (1977).
53. V. B. Lazarev, *Theoret. Exp. Chem.* **3**:294 (1967).
54. L. D. Lucas, *Mem. Sci. Rev. Metallurg.* **61**:1 (1964).
55. A. S. Jordan, *J. Cryst. Growth* **49**:631 (1979).
56. V. M. Glazov, V. B. Kolťsov, and I. R. Suleimanov, *Sov. Phys. Semicond.* **19**:1322 (1985).
57. V. M. Glazov, V. B. Kolťsiv, and V. A. Kurbatov, *Sov. Phys. Semicond.* **22**:202 (1988).
58. V. M. Glazov, S. G. Kim, and K. B. Nurov, *Sov. Phys. Semicond.* **23**:1136 (1989).
59. V. V. Baidov and M. B. Gitis, *Sov. Phys. Semicond.* **4**:825 (1970).
60. V. M. Glazov, S. G. Kim, and T. Suleimanov, *Sov. Phys. Semicond.* **22**:1231 (1988).
61. P. Sommelet and R. L. Orr, *J. Chem. Eng. Data* **11**:64 (1966).
62. B. D. Lichter and P. Sommelet, *Trans. Metallurg. Soc. AIME* **245**:99 (1969).
63. B. D. Lichter and P. Sommelet, *Trans. Metallurg. Soc. AIME* **245**:1021 (1969).
64. *Landolt-Bornstein Numerical Data & Functional Relationship in Science and Technology, New Series, Group 3 Crystal and Solid State Physics, Vol. 17* (1982), p. 16.
65. W. E. Langlois, *J. Cryst. Growth* **56**:15 (1982).
66. K. Kakimoto, P. Nicodème, M. Lecomte, F. Dupret, and M. J. Crochet, *J. Cryst. Growth* **114**:715 (1991).
67. D. R. Hamilton and R. G. Seidensticker, *J. Appl. Phys.* **34**:1450 (1963).
68. Z. Q. Wang, D. Stroud, and A. J. Markworth, *Phys. Rev. B* **40**:3129 (1989).
69. I. Nakatani, K. Masumoto, S. Takahashi, I. Nishida, T. Kiyoawa, and N. Koguchi, *J. Jpn. Inst. Metals* **54**:1025 (1990).

70. K. Kinoshita and T. Yamada, *J. Cryst. Growth* **96**:953 (1989).
71. Y. Malmejac and G. Frohberg, *Fluid Sci. Mater. Sci. Space*, H. U. Walter, ed. (Springer-Verlag, New York, 1987), p. 159.
72. B. Feuerbacher and D. M. Herrlach, 40th Congress IAF, IAF-89-429 (1989).
73. A. Cröll, G. Müller, W. Sebert, and R. Nitsche, *Mater. Res. Bull.* **24**:995 (1989).
74. S. Krishnan, R. H. Hauge, and J. L. Margrave, *Proceedings, Second Noncontact Temperature Measurement Workshop* (Pasadena, Calif., 1989), p. 110.
75. L. N. Hjellming and J. S. Walker, *J. Cryst. Growth* **87**:18 (1988).
76. Z. Q. Wang and D. Stroud, *Phys. Rev. B* **38**:1384 (1988).
77. Z. Q. Wang and D. Stroud, *Phys. Rev. B* **42**:5353 (1990).